

基于湿度刺激响应水凝胶的飞秒激光四维打印研究

邓春三¹, 范旭浩¹, 陶宇峰¹, 焦玢璋¹, 刘耘呈¹, 曲良体², 赵扬³, 李欣⁴, 熊伟^{1*}

¹华中科技大学光学与电子信息学院, 武汉光电国家研究中心, 湖北 武汉 430074;

²清华大学机械工程系, 摩擦学国家重点实验室, 教育部先进材料加工技术重点实验室, 北京 100084;

³北京理工大学化学与化工学院, 原子分子簇科学教育部重点实验室, 光电转换材料北京市重点实验室, 北京 100081;

⁴北京理工大学机械工程学院, 激光微纳加工实验室, 北京 100081

摘要 开发了一种具备湿度刺激响应的复合水凝胶前驱体, 并利用飞秒激光双光子聚合技术, 对该智能响应水凝胶材料进行三维微纳成形制造。系统研究了激光功率和直写速度对该水凝胶材料成形中的线宽、墙高、溶胀度以及机械模量的影响规律, 进一步通过对双层结构的有限元仿真和直写结构的设计, 实现了三维微纳结构在外界环境刺激下的可控形变。理论计算和实验结果表明, 激光功率和直写速度能实现对智能水凝胶材料三维成形和结构性能的精确调制, 实现了双层水凝胶微结构的自主可编程形状转换, 推动了微纳软体机器人和精细组织工程的发展。

关键词 激光光学; 飞秒激光; 双光子聚合; 可编程形变; 智能材料

中图分类号 O343.8

文献标志码 A

doi: 10.3788/CJL202148.0202016

1 引言

智能微型致动器利用外界环境(如温度^[1-2]、酸碱度^[3]、光场^[4]、电场^[5]、磁场^[6-8]等)的刺激变化实现响应性结构变化时, 无需额外的能量系统和复杂的控制系统即可实现可控的操纵, 这对于开发微米级和亚微米级 4D 打印具有重大意义。材料-结构-功能一体化的 4D 打印^[9] 逐渐引发了科学界和产业界的广泛关注。目前微纳结构的 4D 致动手段可主要分为三类。第一类是以异质材料构成的多层结构^[10-12], 这类结构利用不同材料的刺激响应性差异引发结构变形^[11], 可以在多种刺激下实现良好的致动效果和变形, 但是其缺点是对两种及以上异质材料的连接层的牢固度要求较高, 且由于微结构的尺寸限制, 传统的加工制造方法难以实现高精度微致动器的制造; 第二类是通过调控同质材料在不同部位的材料物理化学属性如聚合交联程度等, 诱导差异性的材料刺激响应, 进而实现结构的形变致动^[13], 与第一类型的异质多层结构制造相比, 第二

类制造方法相对简单, 如使用紫外灰度曝光法或变功率激光直写法等可以便利地实现光刻胶材料在三维空间中的交联程度的梯度分布; 第三类方法是利用刺激响应性的分子材料, 如偶氮苯分子的光致异构特性等实现变形致动^[14], 但一般情况下由于制造过程中偶氮苯分子在聚合交联产物中的各向异性, 足够大的变形和致动效果难以在宏观上实现。

飞秒激光双光子聚合技术基于飞秒激光作用下物质的双光子或多光子吸收^[15-16] 实现超光学衍射极限的三维加工, 对未来微纳制造^[17-18]、生物医学工程^[19]、信息存储^[20] 等领域有着重要意义。飞秒激光在智能材料的开发和制造^[21-24] 中已经显现出巨大的吸引力。段宣明课题组^[25] 制造的以牛血清蛋白为基础的三维微结构具有可调制的表面形态和 pH 响应特性; Zhang 等^[26] 通过控制飞秒激光曝光时间和激光扫描步长(200~400 nm) 进而调控聚合物的交联程度, 利用智能材料在不同溶剂下差异性的刺激响应, 制造出可控形变的智能微执行器; 段慧玲课题组^[27] 通过双光子聚合技术, 以丙烯酸和异丙基丙

收稿日期: 2020-08-31; 修回日期: 2020-09-30; 录用日期: 2020-11-05

基金项目: 国家重点研发计划(2017YFB1104300)、国家自然科学基金面上项目(61774067)、中央高校基本科研业务费专项资金(2017KFXKJC001, 2018KFYXKJC027)、国家博士面上基金(2017M622417)

*E-mail: weixiong@hust.edu.cn

烯酰胺为功能单体,成功设计出具有外部环境响应功能的智能微铰链结构单元,其中基于不同激光功率加工的微纳双层梁结构可在外部环境 pH 激励下实现可控变形。然而,基于湿度的微纳结构刺激响应致动鲜有报道,与其他刺激方式相比,湿度刺激易于微环境集成,系统简单易控,适用范围更广。孙洪波课题组^[28]利用飞秒激光成形聚乙二醇二丙烯酸酯,发现直写成形的结构具备良好的吸水溶胀特性,但未做致动器的四维打印研究;Takuzo Aida 课题组^[29]将碳酸胍(Gdm_2CO_3)作为起始化合物,利用与玻璃基板形成的 π 堆叠氮化碳聚合物(CNP)制备出致动薄膜,该薄膜因对水的吸附和解吸作用迅速弯曲甚至出现垂直跳跃^[29];刘笔锋课题组^[30]通过在氧化石墨烯(GO)薄膜上微压印图案化的聚吡咯(PPY),制备出 GO/PPY 双层不对称可编程智能执行器,利用水分子的吸附/解吸原理实现了出色的致动性能。理论上,通过调谐激光参数,飞秒激光直写技术能将具有预定义的交联梯度的智能材料以亚微米分辨率打印形成任意复杂的 3D 结构,因此在微纳尺度刺激响应致动器方面有着巨大的应用前景。然而目前适用飞秒激光直写三维成形的智能材料依然面临着材料种类单一,材料成形过程中激光直写工艺参数对智能材料的成形精度以及成形后的材料性能的影响缺乏系统研究,智能微结构设计缺乏理论指导等问题,阻碍了未来复杂的微致动功能器件的物理实现与应用发展。

本文开发了一种新型光固化智能水凝胶材料,该材料适用于飞秒激光直写成形,并具有优秀的湿度刺激响应性。基于此材料系统研究了成形结构的形貌尺寸、溶胀度以及机械模量随激光功率和直写速度的变化规律。通过调谐激光参数,直写具有不同聚合交联程度的双层同质材料的网状微结构,实现了湿度刺激下三维微结构可控且可逆的弯曲、卷曲等自驱动功能;并通过建立对应材料的数理模型,利用有限元仿真预测了微纳结构的三维结构形变,仿真结果与实际实验结果具有较好的吻合度。基于有限元理论仿真和双光子聚合三维打印,可以成功设计并制备出多种如含羞草、六叶花瓣的可编程仿生结构,这些结构可以在外部湿度刺激下快速、精确、可逆地转换为预定义形变。这种基于智能材料的飞秒激光直写制造技术可对未来具备环境刺激响应性的自驱动智能微纳机器人等微纳功能器件的研发提供一条可行路径。

2 实验材料与方法

2.1 实验材料

实验中采用聚乙二醇二丙烯酸酯(PEGDA575)(Sigma-Aldrich, St. Louis, MO, USA)、异丙基丙烯酸酰胺(NIPAAm)(Sigma-Aldrich, St. Louis, MO, USA)作为成链单体;采用亚甲基蓝(MB)作为双光子聚合光引发剂,用于荧光成像;采用乙二醇(EG)溶剂。所有试剂购买后直接使用,具体化学分子结构如图 1(a)所示。

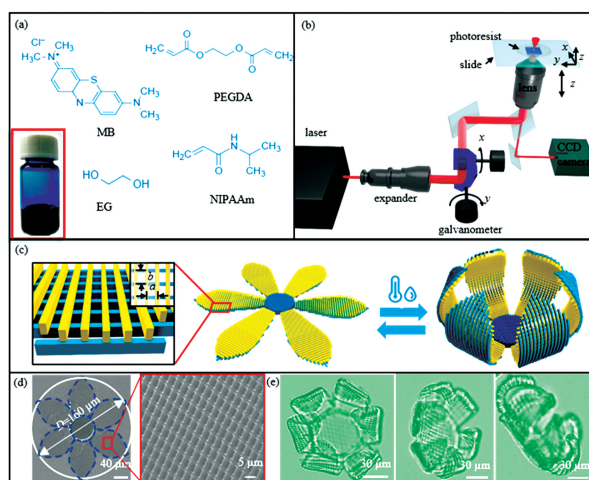


图 1 智能材料微纳结构的直写成形。(a)光刻胶的组成,插图为实际样品照片;(b)飞秒激光双光子聚合用于三维加工示意图;(c)不同线间距的网状结构和形状转换;(d)六瓣花瓣网状双层结构;(e)六瓣花瓣微结构在水环境下的自弯曲形状转换图

Fig. 1 Direct writing of micro-nano structure of smart materials. (a) Chemical molecular structure of the composition of the photoresist and a photo of an actual sample; (b) schematic diagram of femtosecond two-photon polymerization system used to 3D processing; (c) schematic of double-layer mesh structure with different line spacing and its shape transformation; (d) SEM image of the double-layer six-petal structure; (e) shape transformation diagram of the self-bending six-petal structure in water

2.2 实验方法

实验中采用的飞秒激光器 (COHERENT, Chameleon Discovery) 的波长为 780 nm, 脉冲宽度为 100 fs, 入射激光通过扩束镜准直后进入振镜 (Thorlabs, GVS012/M) 在 XY 平面上进行扫描, 经过振镜的光束被引入显微物镜 (60×油镜) 进而聚焦产生椭球形聚焦点, 在激光辐照下, 处于焦点中心处的光刻胶会发生双光子聚合固化反应, 结合振镜及三维位移平台 (Physik Instrumente, P-563.3CD) 即可实现 XYZ 空间的三维成形制造。其中系统加工光路如图 1(b) 所示。

系统研究了不同激光功率和直写速度下单位水凝胶模型的线宽和墙高变化, 利用微纳力学测试系统 (Femto Tools AG, FT-MTA 02) 采集成形材料的应力应变, 在光学显微镜 (Olympus, IX83) 下观察施加刺激后成形结构的溶胀度变化及形状转换。如图 1(c) 所示, 针对同质水凝胶双层结构, 控制两层结构中各自的线间距 a, b 并调谐飞秒激光直写功率和直写速度控制材料的交联程度, 进而控制材料的刺激响应性, 实现结构自弯曲或自卷曲动作。图 1(d) 和图 1(e) 展示了设计加工的网状六瓣花瓣结构 (直径 $D=160 \mu\text{m}$) 的自弯曲形状转换。

2.3 实验原理

激光诱导材料的形成机理是基于飞秒激光双光子聚合原理, 在 780 nm 波长的飞秒激光作用下, 光引发剂亚甲基蓝同时吸收两个光子能量完成跃迁产

生活性自由基, 进而引发单体打开材料的不饱和化学键 (碳碳双键) 形成大分子自由基进行链增长, 最终由两个自由基的相互作用, 终止链增长, 聚合成链。湿度刺激响应是两个单体材料 (聚乙二醇二丙烯酸酯和异丙基丙烯酰胺) 在水环境下, 基于亲水基团的亲水性, 水分子进入聚合物交联网络, 导致结构发生溶胀。

3 分析与讨论

3.1 不同激光直写参数下智能水凝胶成形线宽及墙高分析

飞秒激光双光子聚合直写结构的成形精度主要和激光光强、直写速度以及材料的聚合阈值功率等参数有关。为系统研究智能水凝胶的成形精度随激光直写参数的变化规律, 选择在 10~35 mW 的激光功率和 100~1000 $\mu\text{m}/\text{s}$ 的直写速度范围内通过双光子聚合加工跨度为 10 μm 的单线悬臂结构, 利用扫描电子显微镜测量单根悬线的横向线宽和纵向墙高并进行统计对比, 具体结果如图 2 所示。实验结果表明, 水凝胶成形线宽和墙高受激光功率和直写速度的影响较大。在相同激光功率下, 悬线成形线宽和墙高随着扫描速度的减小逐渐增加, 如: 在激光功率为 20 mW, 直写速度 1000 $\mu\text{m}/\text{s}$ 时, 得到能够自支撑的单线悬臂的最小线宽为 400 nm, 最小墙高为 400 nm; 而当直写速度降低至 100 $\mu\text{m}/\text{s}$ 时, 悬臂线宽达到 1.25 μm , 墙高达到 1.5 μm 。这主要是由

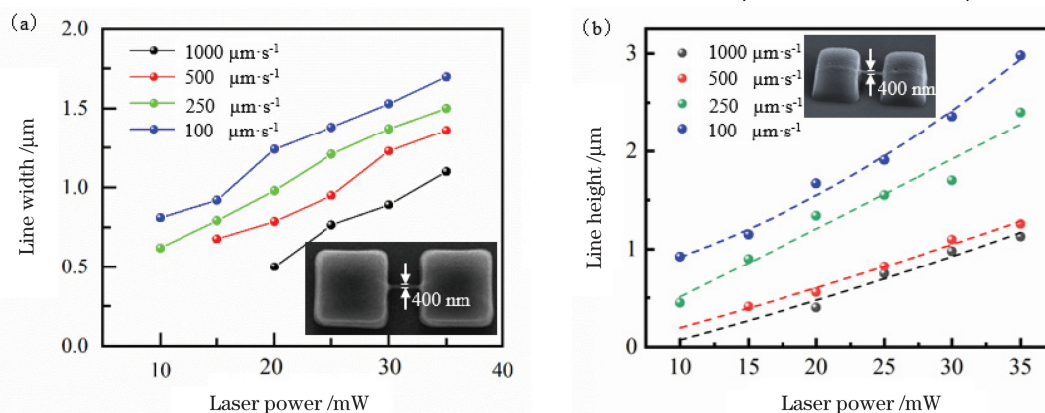


图 2 不同激光功率和直写速度下, 悬线模型线宽和墙高的变化规律。(a) 线宽变化曲线图, 插图为激光功率为 20 mW, 加工速度为 1000 $\mu\text{m} \cdot \text{s}^{-1}$ 时的单线悬臂电子显微镜图, 悬线跨度尺寸为 10 μm ; (b) 墙高变化曲线图, 插图为激光功率为 20 mW, 加工速度为 1000 $\mu\text{m} \cdot \text{s}^{-1}$ 时单线悬臂在 45° 下的电子显微镜图

Fig. 2 Dependence of the width and height of suspension beam model on laser power and scanning speed. (a) Diagram of line width with respective to the laser power and scanning speed, in which the inset shows the SEM image of the suspended cantilever fabricated under the laser power of 20 mW and scanning speed of 1000 $\mu\text{m} \cdot \text{s}^{-1}$; (b) diagram of line height with respective to the laser power and scanning speed, in which the inset shows the 45° titled SEM image of the suspended cantilever

于在同样激光功率下,较低的激光直写速度延长了材料的曝光时间,从而在聚合过程中产生更多的自由基,成形尺寸增大。在相同直写速度下,随着激光功率的增加,成形线宽和墙高显著增加,如:100 $\mu\text{m}/\text{s}$ 的直写速度下,激光功率为 15 mW 时,成形线宽为 870 nm,墙高为 1.1 μm ;而当激光功率提高至 35 mW 时,线宽达到实验的最大值 1.7 μm ,墙高最大值为 3 μm 。这是由于飞秒激光光束截面光强呈高斯型函数分布,在直写速度和材料双光子吸收阈值一定时,随着激光功率的增加,材料内发生双光子吸收的范围增加,实验结果符合预期。

3.2 不同激光直写参数下材料溶胀度研究分析

水凝胶的聚合程度受激光工艺参数的影响较大,这对于智能水凝胶的材料性能至关重要,故测试了外界环境刺激下不同激光功率和直写速度对三维水凝

胶微结构的溶胀度,见图 3。一方面为了减小结构与衬底之间黏附带来的溶胀影响,另一方面为了节省加工时间,保证空间溶胀的各向同性,方便体积溶胀度测试,设计了一个球径为 40 μm 的中空足球三维微结构研究模型,系统研究了其在去离子水环境下的溶胀现象。其中,为减小微结构与衬底之间的黏接影响,足球底部设置了一个直径为 40 μm 的支撑底座,具体形貌如图 3(b) 所示。实验中,在微结构上滴加去离子水后,足球模型迅速吸水溶胀,其球径由 d_0 溶胀增大至 D_t ,利用光学显微镜记录不同直写参数下的足球直径变化,该参数下的体积溶胀度可表示为

$$W_R = \frac{V_t - V_0}{V_0} = \frac{D_t^3 - d_0^3}{d_0^3}, \quad (1)$$

式中: V_0 为干燥状态下的足球体积; V_t 为施加去离子水后的足球溶胀体积。

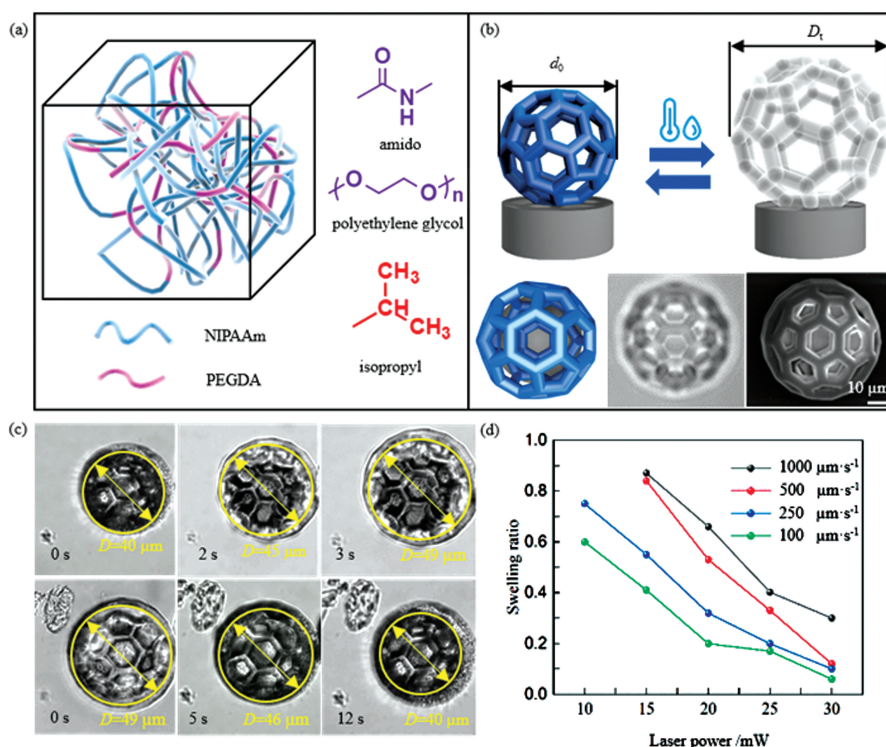


图 3 水凝胶材料在不同直写参数下的溶胀度测试。(a) 单体材料由链式聚合形成三维网络示意图以及单体材料中刺激响应性基团化学结构式;(b) 足球溶胀示意图;(c) 激光功率为 15 mW、扫描速度为 500 $\mu\text{m} \cdot \text{s}^{-1}$ 下所制备的足球模型的溶胀、消溶胀的显微光学图片;(d) 不同激光直写参数下水凝胶足球模型的溶胀度变化规律图

Fig. 3 Swelling degree test of hydrogel materials under different direct writing parameters. (a) Three-dimensional network diagram of the monomer material formed by chain polymerization and the chemical structural formula of the stimulus responsive group existing in the monomer material; (b) schematic diagram of football swelling; (c) optical microscope image of football model during swelling and de-swelling process under laser power of 15 mW and scanning speed of 500 $\mu\text{m} \cdot \text{s}^{-1}$; (d) swelling degree of hydrogel football model under different laser direct writing process parameters

如图 3(a) 所示,聚合单体异丙基丙烯酰胺中存在的丙烯酰胺基和聚乙二醇二丙烯酸酯存在的聚乙

二醇基团,在常温下均具备优异的亲水性能。在双光子直写过程中,单体材料存在的饱和化学键会

断裂形成高分子链并互相交联形成复杂的三维网络,而该三维网络的形成可为水分子提供足够空间,因此在亲水基团的作用下可以吸收容纳大量的水分子进而引起三维网络微结构溶胀。如图 3(c)所示,在激光功率为 15 mW,直写速度为 500 $\mu\text{m}/\text{s}$ 的情况下,水凝胶足球模型达到溶胀平衡仅需 3 s,溶胀后足球体积为原体积的 1.84 倍,溶胀比达到 84%;进一步蒸发水分,足球模型可在 12 s 内消溶胀恢复至原始体积,这为自致动微结构设计提供了可能。调谐激光功率和直写速度,改变智能材料聚合过程中三维网络结构的聚合交联程度,可使足球的体积溶胀度存在显著差异,具体的溶胀度变化曲线如图 3(d)所示:在相同直写速度下,随着激光功率的增加,聚合加工成形的结构的溶胀度急剧减小,当激光功率达到一定值时,较高的材料聚合程度可使加工的结构基本不再具有溶胀性质,如激光功率为 25 mW,扫描速度为 500 $\mu\text{m}/\text{s}$ 时,足球的球径可溶胀到 44 μm ,溶胀度为 33%,而当激光功率增加至 30 mW 时,结构的溶胀度减小为 13%;在相同激光功率下,足球溶胀度随着直写速度的增加逐渐减小,如激光功率为 20 mW 时,随着直写速度从 100 $\mu\text{m}/\text{s}$ 增加到 1000 $\mu\text{m}/\text{s}$ 中,足球模型的溶胀度从 21%增大至 68%。

通过上述分析发现,自主开发的智能水凝胶材料的溶胀度在不同激光直写参数下的变化明显,可用于实现智能材料溶胀程度的精细调控。并且相较于宏观尺度,微观尺度下模型的表面积和体积之比

更大,因此微纳结构将无疑具有更快的响应速度,这将有助于微纳智能响应器件的快速自驱动形变等应用。

3.3 不同激光直写参数下材料机械模量的研究分析

为研究水凝胶材料的机械模量在飞秒激光直写下的可控性,对不同激光直写参数下所制备的 100 $\mu\text{m} \times 100 \mu\text{m} \times 30 \mu\text{m}$ 的水凝胶长方体块进行了应力应变测试,测试过程中保持激光直写过程中结构的层间距(400 nm)和线间距(400 nm)不变。采用微纳力学测试系统进行测试,其压头为端面 50 $\mu\text{m} \times 50 \mu\text{m}$ 的梯形压头,设置最大载荷为 10 mN,加载速度为 0.05 $\mu\text{N}/\text{s}$,测试环境温度为 20 $^{\circ}\text{C}$,相对湿度为 45%。该测试系统利用力学探针通过加载力的方式测量力与位移之间的关系曲线,如图 4(a)所示为不同激光直写参数下所形成的水凝胶材料的位移-力曲线,其中实线表示压头加载曲线,虚线表示卸载曲线。从图中可以看出,在 0~10 mN 范围内,材料的弹性性能良好,且在压力卸载过程中具有良好的弹性往复能力;当压力加载到最大压力的时候,压入深度随着激光功率的增加逐渐减小。利用微力学测试系统采集的位移-力数据,在材料弹性形变范围内,取曲线上的力变化量以及对应的位移差,两者之间的比值作为对应实验参数下的结构刚度,即

$$K_{\text{stiffness}} = \Delta F / \Delta h, \quad (2)$$

式中: F 为作用于立方块上的压力; h 为由于力而产生

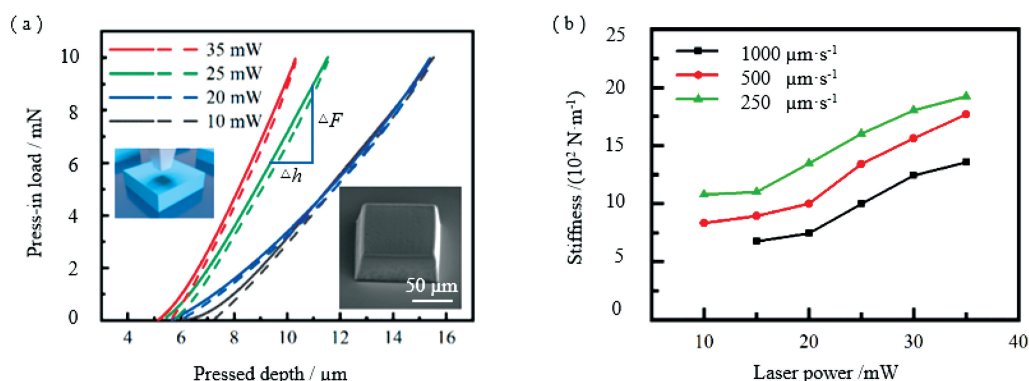


图 4 不同激光直写参数下水凝胶材料的机械模量变化规律。(a)在 250 $\mu\text{m} \cdot \text{s}^{-1}$ 扫描直写速度下,采用不同激光功率形成的水凝胶材料的应力应变曲线图(实线表示压头加载曲线,虚线表示卸载曲线),右下插图为测试块的扫描电子显微镜图;(b)不同激光直写参数下水凝胶材料的机械模量测试结果

Fig. 4 Variation of mechanical modulus of hydrogel materials under different laser direct-writing parameters. (a) Stress-strain curves of hydrogel materials formed under different laser powers at a scanning direct writing speed of 250 $\mu\text{m} \cdot \text{s}^{-1}$ (the solid line represents the loading curve of the head and the dotted line represents the unloading curve), and a scanning electron microscope image of the test block; (b) test results of mechanical modulus of hydrogel materials under different laser direct-writing parameters

生的弹性应变。

图 4(b)展示了不同激光直写参数下水凝胶材料的机械模量变化曲线,在相同的直写速度下,材料机械模量会随着激光功率的增加显著增大,如在激光功率为 15 mW,1000 $\mu\text{m}/\text{s}$ 的扫描速度下,材料机械模量最小为 676 N/m,当激光功率在 35 mW,扫描速度降低至 250 $\mu\text{m}/\text{s}$ 时,材料刚度增加至 1923 N/m。上述结果充分说明通过调谐飞秒激光直写工艺参数可以实现对材料机械模量的有效调控。

3.4 水凝胶可编程制动微结构的设计与激光直写成形

上述实验结果表明,调谐激光功率和直写速度可以控制湿度刺激响应水凝胶的成形线宽和墙高以及成形结构的溶胀度和机械模量的变化。因此可以利用改变飞秒激光双光子聚合加工参数的方式,使打印成形的刺激响应性水凝胶三维微结构具备可编程的形状转换能力。为了实现这一目标,利用飞秒激光双光子聚合直写技术设计并加工如图 5(a)所示的双层网状结构。第一层直写路径与 X 轴正方向夹角定义为 α ,第二层直写路径与 X 轴正方向夹角定义为 β ,具体直写参数选择如表 1 所示。由于网状微结构上下两层的溶胀度和机械模量的不同,在显影后的网状微结构上滴加去离子水,微结构迅速做出弯曲动作;进一步为了验证激光直写路径对结构致动方向的影响,改变第一层和第二层直写路径夹角如表 2 所示,在所打印出的微结构上滴加去离子水后,双层网状微结构发生了自卷曲动作,值得

注意的是,网状微结构的弯曲和卷曲均是可逆的。利用有限元仿真软件 ABAQUS 计算得到的结构仿真结果与实验结果具有良好的 consistency。为进一步验证改变激光直写参数可以定量调节双层网状微结构的弯曲角度($90^\circ \pm 10^\circ$ 和 $180^\circ \pm 10^\circ$),如图 5(c)所示,利用已建立的结构数理模型得到符合条件(溶胀度、机械模量)所对应的直写工艺参数,并设计第一层和第二层网状结构的激光直写路径,制备了一个六叶花瓣模型。实验结果显示,在显影后的微结构上滴加去离子水,相同结构的六叶花瓣可得到与理论设计结果相一致的自弯曲效果且弯曲角度可控。为了验证结果的可逆性和稳定性,在湿度环境和干燥环境下循环刺激重复测量 50 次,实验结果表明结构具有良好的可重复性,得到的弯曲和卷曲角度误差在 $\pm 10^\circ$ 范围内。上述方法不仅适用于六叶花瓣模型,还可适用于更复杂的结构成形制造。受大自然的启发,如含羞草在外界刺激下能实现同一藤蔓不同长度叶子的自闭合以保护自己免受风雨摧折,本课题组设计了长宽高为 $200 \mu\text{m} \times 250 \mu\text{m} \times 4 \mu\text{m}$ 的仿生含羞草结构,具体结果如图 5(d)所示。直写成形后的含羞草结构,在滴加 100 μL 去离子水刺激后,不同长度的叶子会迅速做出相同角度的自闭合动作转换,并在去水干燥的环境下,能恢复成铺展开状态。综上,利用材料有限元数理模型和工艺参数,可以面向功能需求来选择合适的激光直写参数进行激光制造,这为通过飞秒激光四维打印技术实现三维微结构功能器件的应用提供了一种科学方法。

表 1 自弯曲结构飞秒激光直写参数

Table 1 Femtosecond laser direct writing parameters for self-bending transformation

Layer	Laser power /mW	Scanning speed /($\text{mm} \cdot \text{s}^{-1}$)	Scanning angle /($^\circ$)	Line spacing / μm
Layer 1	15	0.5	0	4
Layer 2	20	0.5	90	3

表 2 自卷曲结构飞秒激光直写参数

Table 2 Femtosecond laser direct writing parameters for self-curling transformation

Layer	Laser power /mW	Scanning speed /($\text{mm} \cdot \text{s}^{-1}$)	Scanning angle /($^\circ$)	Line spacing / μm
Layer 1	10	0.25	60	4
Layer 2	25	0.5	90	3

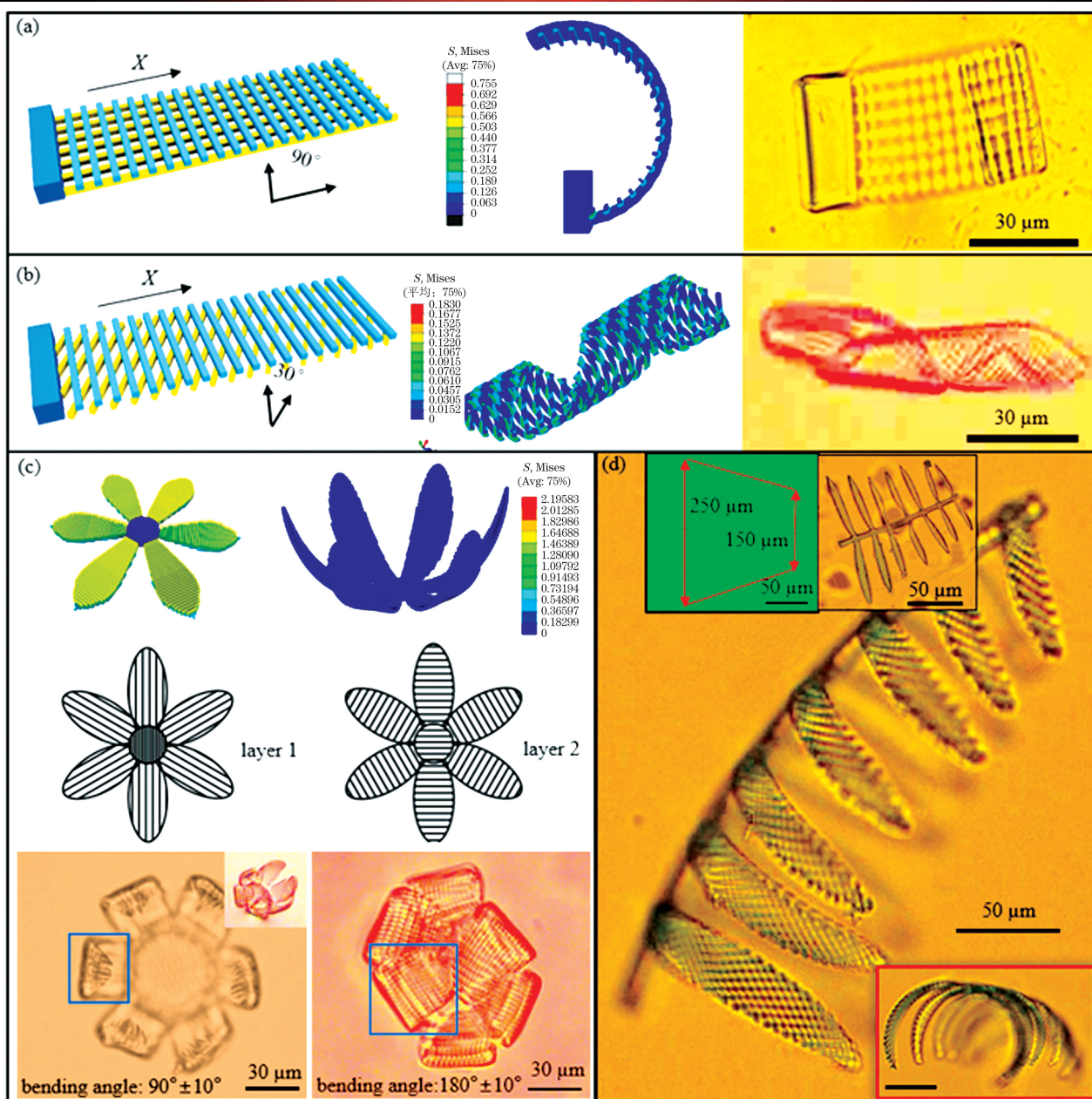


图 5 双层致动微结构的设计、制造与测试。(a)(b)基于有限元仿真计算得到的双层带状微结构的自弯曲和自卷曲的形貌图及其实验结果。(c)采用不同的激光直写参数可以获得不同自弯曲效果;(d)仿生含羞草微结构设计和激光直写制造效果图,左上角分别是飞秒激光直写后未显影和显影后的结构显微光学图片

Fig. 5 Design, manufacturing and testing of the double-layer actuation microstructure. (a)(b) Self-bending and self-curling topography of the double-layer ribbon microstructure based on finite element simulation calculations and corresponding experimental results; (c) different self-bending effects obtained using different laser direct writing parameters; (d) microstructure design of bionic mimosa and the effect of laser direct writing manufacturing, and the upper left corner is the undeveloped and developed microscopic optical pictures of the structure after femtosecond laser direct writing

4 结 论

微纳 4D 打印可用于开发具有感知-决策-响应功能的一体化微纳智能器件,在生物医疗,组织工程、微机械和软体机器人等领域有着巨大的应用前

景。本研究开发了一种对水环境敏感、适用于飞秒激光双光子聚合直写的复合水凝胶材料,系统研究了不同激光功率、直写速度工艺对材料聚合加工成形的线宽、墙高、溶胀度以及材料机械模量的变化规律。在激光直写成形的制造参数范围内,可实现最小

线宽为 400 nm, 最小墙高为 400 nm, 以及最高溶胀度为 84% 的水凝胶微纳结构。通过调谐激光功率、直写速度以及扫描路径, 所设计的双层网状微结构能够快速响应水环境刺激, 实现自弯曲和自卷曲的可逆形变。进一步建立双层结构的数理模型并应用有限元计算仿真和实验测试验证了从拓扑结构设计到目标功能实现的科学方法, 实现了六叶花瓣结构和含羞草结构的飞秒激光微纳打印, 获得了可编程控制的可逆 3D 形状转换功能, 为将来微纳软机器人、微纳传感和制动功能器件的开发和应用提供了参考。

参 考 文 献

- [1] Hippler M, Blasco E, Qu J, et al. Controlling the shape of 3D microstructures by temperature and light [J]. *Nature Communications*, 2019, 10(1): 232.
- [2] Zolfagharian A, Kaynak A, Khoo S Y, et al. Pattern-driven 4D printing[J]. *Sensors and Actuators A: Physical*, 2018, 274: 231-243.
- [3] Baldi A, D'Aniello P, Giuliano G, et al. Behavior of lipoprotein X (LP-X) in viral hepatitis[J]. *Quaderni Sclavo di Diagnostica Clinica e di Laboratorio*, 1975, 11(1): 122-130.
- [4] Davidson E C, Kotikian A, Li S C, et al. 3D printable and reconfigurable liquid crystal elastomers with light-induced shape memory via dynamic bond exchange[J]. *Advanced Materials*, 2020, 32(1): 1905682.
- [5] Han D, Farino C, Yang C, et al. Soft robotic manipulation and locomotion with a 3D printed electroactive hydrogel[J]. *ACS Applied Materials & Interfaces*, 2018, 10(21): 17512-17518.
- [6] Behl M, Razaq M Y, Lendlein A. Multifunctional shape-memory polymers [J]. *Advanced Materials*, 2010, 22(31): 3388-3410.
- [7] Peters C, Hoop M, Pané S, et al. Degradable magnetic composites for minimally invasive interventions: device fabrication, targeted drug delivery, and cytotoxicity tests [J]. *Advanced Materials*, 2016, 28(3): 533-538.
- [8] Buguin A, Li M H, Silberzan P, et al. Micro-actuators: when artificial muscles made of nematic liquid crystal elastomers meet soft lithography[J]. *Journal of the American Chemical Society*, 2006, 128(4): 1088-1089.
- [9] Shi Y S, Wu H Z, Yan C Z, et al. Four-dimensional printing: the additive manufacturing technology of intelligent components [J]. *Journal of Mechanical Engineering*, 2020, 56(15): 1-25.
史玉升, 伍宏志, 闫春泽, 等. 4D 打印: 智能构件的增材制造技术 [J]. *机械工程学报*, 2020, 56(15): 1-25.
- [10] Zhao Z A, Kuang X, Yuan C, et al. Hydrophilic/hydrophobic composite shape-shifting structures [J]. *ACS Applied Materials & Interfaces*, 2018, 10(23): 19932-19939.
- [11] Ji Z Y, Yan C Y, Yu B, et al. 3D printing of hydrogel architectures with complex and controllable shape deformation [J]. *Advanced Materials Technologies*, 2019, 4(4): 1800713.
- [12] Montero de Espinosa L, Meesorn W, Moatsou D, et al. Bioinspired polymer systems with stimuli-responsive mechanical properties [J]. *Chemical Reviews*, 2017, 117(20): 12851-12892.
- [13] Li C S, Lo C W, Zhu D F, et al. Synthesis of a photoresponsive liquid-crystalline polymer containing azobenzene [J]. *Macromolecular Rapid Communications*, 2009, 30(22): 1928-1935.
- [14] Liu J, Wang M L, Wu X H, et al. Barrier property of polarized light oriented azobenzene containing side-chain liquid crystalline polymer [J]. *Acta Polymerica Sinica*, 2011(7): 729-734.
刘剑, 王明乐, 吴晓华, 等. 光致取向调控偶氮苯侧链液晶聚合物的阻隔特性研究 [J]. *高分子学报*, 2011(7): 729-734.
- [15] Qin H L, Zhang T, Li N, et al. Anisotropic and self-healing hydrogels with multi-responsive actuating capability [J]. *Nature Communications*, 2019, 10: 2202.
- [16] Rao S L, Wu P C, Zhang C C, et al. Energy-controllable femtosecond laser fabrication based on spatial light modulator [J]. *Chinese Journal of Lasers*, 2017, 44(1): 0102008.
饶生龙, 吴培超, 张晨初, 等. 基于空间光调制器的能量可控飞秒激光加工 [J]. *中国激光*, 2017, 44(1): 0102008.
- [17] del Barrio J, Sánchez-Somolinos C. Light to shape the future: from photolithography to 4D printing [J]. *Advanced Optical Materials*, 2019, 7(16): 1900598.
- [18] Shi Y, Xu B, Wu D, et al. Research progress on fabrication of functional microfluidic chips using femtosecond laser direct writing technology [J]. *Chinese Journal of Lasers*, 2019, 46(10): 1000001.
史杨, 许兵, 吴东, 等. 飞秒激光直写技术制备功能化微流控芯片研究进展 [J]. *中国激光*, 2019, 46(10): 1000001.
- [19] Stroganov V, Pant J, Stoychev G, et al. 4D biofabrication: 3D cell patterning using shape-changing films [J]. *Advanced Functional Materials*, 2018, 28(11): 1706248.
- [20] Huang L M, Jiang R Q, Wu J J, et al. Ultrafast digital printing toward 4D shape changing materials [J]. *Advanced Materials*, 2017, 29(7): 1605390.
- [21] Liu Y, Xiong W, Li D W, et al. Precise assembly

- and joining of silver nanowires in three dimensions for highly conductive composite structures [J]. *International Journal of Extreme Manufacturing*, 2019, 1(2): 025001.
- [22] Li J J, Liu Y, Qu S L. Research progress on optical fiber functional devices fabricated by femtosecond laser micro-nano processing [J]. *Laser & Optoelectronics Progress*, 2020, 57(11): 111402.
李金健, 刘一, 曲士良. 飞秒激光微纳加工光纤功能器件研究进展[J]. *激光与光电子学进展*, 2020, 57(11): 111402.
- [23] Cao X W, Zhang L, Yu Y S, et al. Application of micro-optical components fabricated with femtosecond laser [J]. *Chinese Journal of Lasers*, 2017, 44(1): 0102004.
曹小文, 张雷, 于永森, 等. 飞秒激光制备微光学元件及其应用[J]. *中国激光*, 2017, 44(1): 0102004.
- [24] Liu M N, Li M T, Sun H B. 3D femtosecond laser nanoprinting[J]. *Laser & Optoelectronics Progress*, 2018, 55(1): 011410.
刘墨南, 李木天, 孙洪波. 3D 飞秒激光纳米打印[J]. *激光与光电子学进展*, 2018, 55(1): 011410.
- [25] Wei S, Liu J, Zhao Y, et al. Protein-based 3D microstructures with controllable morphology and pH-responsive properties[J]. *ACS Applied Materials & Interfaces*, 2017, 9(48): 42247-42257.
- [26] Zhang Y L, Tian Y, Wang H, et al. Dual-3D femtosecond laser nanofabrication enables dynamic actuation[J]. *ACS Nano*, 2019, 13(4): 4041-4048.
- [27] Jin D D, Chen Q Y, Huang T Y, et al. Four-dimensional direct laser writing of reconfigurable compound micromachines [J]. *Materials Today*, 2020, 32: 19-25.
- [28] Lü C, Sun X C, Xia H, et al. Humidity-responsive actuation of programmable hydrogel microstructures based on 3D printing[J]. *Sensors and Actuators B: Chemical*, 2018, 259: 736-744.
- [29] Arazoe H, Miyajima D, Akaike K, et al. An autonomous actuator driven by fluctuations in ambient humidity[J]. *Nature Materials*, 2016, 15(10): 1084-1089.
- [30] Dong Y, Wang J, Guo X, et al. Multi-stimuli-responsive programmable biomimetic actuator [J]. *Nature Communications*, 2019, 10(1): 4087.

Femtosecond Laser Four-Dimensional Printing Based on Humidity Responsive Hydrogels

Deng Chunsan¹, Fan Xuhao¹, Tao Yufeng¹, Jiao Binzhang¹, Liu Yuncheng¹, Qu Liangti², Zhao Yang³, Li Xin⁴, Xiong Wei^{1*}

¹ School of Optical and Electronic Information, Wuhan National Laboratory for Optoelectronics, Huazhong University of Science and Technology, Wuhan, Hubei 430074, China;

² Department of Mechanical Engineering, State Key Laboratory of Tribology, Key Laboratory for Advanced Materials Processing Technology, Tsinghua University, Beijing 100084, China;

³ School of Chemistry and Chemical Engineering, Key Laboratory of Cluster Science, Ministry of Education, Beijing Key Laboratory of Photoelectronic/Electrophotonic Conversion Materials, Beijing Institute of Technology, Beijing 100081, China;

⁴ School of Mechanical Engineering, Laser Micro/Nano Fabrication Laboratory, Beijing Institute of Technology, Beijing 100081, China

Abstract

Objective Intelligent hydrogels usually exhibit environmental stimulus responsiveness when the external environment changes based on a unique three-dimensional network formed by cross-linking with chemical bonds or physical interactions, which makes it play an essential role in biomedicine, tissue engineering, soft robotics, and other fields. The femtosecond laser direct-writing (FLDW) technology based on the principle of two-photon nonlinear absorption has the advantages of nanoscale resolution. It also has three-dimensional modeling capabilities which are difficult to realize by UV lithography, electron beam etching, or nanoimprint. However, FLDW technology is still facing challenges in manufacturing smart micro-nanostructure devices, such as a single smart material system that meets the femtosecond laser manufacturing requirements. These include the lack of systematic research on the influence of FLDW process parameters on the manufacturing accuracy of intelligent materials and properties of manufactured materials, and lack of theoretical guidance in smart microstructures' design. In this

study, we developed a composite intelligent hydrogel and applied the two-photon polymerization (TPP) technique to achieve four-dimensional microscale printing. We investigated the effects of femtosecond laser power and scanning speed on the line width, line height, swelling ratio, and hydrogels' mechanical modulus. We realized the controllable transformation of the three-dimensional micro-nanostructure under external environmental stimuli using the finite element simulation. Theoretical calculation and experimental results show that the controllable modulation of the three-dimensional shaping and structural performance of the smart hydrogel material can be realized using the laser parameters. However, the double-layer hydrogel microstructure can achieve the autonomous programmable transformation. This work laid a foundation for the development of soft-robots and tissue engineering.

Methods First, we manufacture smart photoresist materials composed of smart monomers, crosslinkers, and photoinitiators using the FLDW platform based on the principle of two-photon nonlinear absorption that can achieve three-dimensional manufacture with nanoresolution. A single suspension wire with a pitch of $10\ \mu\text{m}$ is manufactured to measure the line width and height using a scanning electron microscope. The volume swelling degree is tested under an optical microscope using a football model with a diameter of $40\ \mu\text{m}$. The law between the volume swelling degree and the laser manufacturing parameters is studied. In the next step, we use the micromechanics testing system (Femto Tools AG, FT-MTA 02) to test the stress and strain of the $100\text{-}\mu\text{m} \times 100\text{-}\mu\text{m} \times 30\text{-}\mu\text{m}$ cuboid and obtain the law of stiffness with the FLDW parameters. Combined with the finite element simulation calculations and experiments, the designed double-layer network structure has excellent self-driving performance in the presence or absence of a water environment. The reversible deformation is repeatedly measured 50 times under an optical microscope, and the average error is counted to ensure the universality of the results.

Results and Discussions The configured intelligent photoresist material with a certain proportion of intelligent monomers, cross-linkers, and initiators could meet the femtosecond laser TPP manufacturing requirements. Both the minimum line width and minimum line-height can reach $400\ \text{nm}$ within the forming range. In general, with the increase of laser power and decrease of direct-writing speed, line width and line-height increase accordingly (Fig. 2). The unit model's swelling degree study shows that the swelling degree changes obviously under the premise of satisfying the laser power forming and direct writing speed. In this study, the maximum volume swelling degree can achieve 84% , and minimum swelling degree is only one-tenth of the maximum, which makes it possible for the structure to be self-driving (Fig. 3). Since different laser powers and direct writing speeds will make the degree of crosslinking of organic materials in the polymerization process different, the structure's mechanical modulus after manufacturing will also be different. In the mechanical modulus test, it can be seen that with the change of laser power and direct writing speed, stiffness has the same trend as line width, line height, and swelling degree. The stiffness can reach a minimum of $676\ \text{N/m}$ when the laser power is $15\ \text{mW}$, and the direct writing speed is $1000\ \mu\text{m/s}$. When the laser power is increased to $35\ \text{mW}$ and scanning speed is reduced to $250\ \mu\text{m/s}$, the modulus of $1923\ \text{N/m}$ can be achieved (Fig. 4). Since the laser direct writing parameters have such significant influence on material manufacturing, the mesh structure manufactured by tuning the parameters has an excellent self-driving function (Fig. 5).

Conclusions In this study, we developed a composite hydrogel material sensitive to the water environment and suitable for femtosecond laser direct-writing. The study obtained the change law of the line width, wall height, swelling degree, and material mechanical modulus at different laser powers and direct writing speeds. Within the manufacturing parameters of laser direct-writing, the material could be shaped to achieve the minimum line width of $400\ \text{nm}$, 400-nm minimum high wall, and micro-nano structure with a maximum swelling degree of 84% . The double-layer mesh microstructure with different laser powers, direct writing speeds, and scanning paths could quickly respond to water environment stimuli, proving that the reversible deformation of self-bending and self-curling is feasible. Furthermore, we established the double-layer structure's mathematical model and applied the finite element calculation simulation to verify the scientific method from topology design to target function realization. We realized the reversible 3D shape conversion function of programmable control of the six-leaf petal structure and mimosa structure. These studies have laid the foundation for developing and applying micro-nano soft robots, micro-nanosensing, and functional braking devices in the future.

Key words laser optics; femtosecond laser; two-photon polymerization; programmable transformation; intelligent materials

OCIS codes 140.3460; 020.4180; 350.6980; 160.5470